

# A novel method for fabrication of CdS quantum dot-sensitized solar cells

Yu Zhang<sup>1,2</sup> · Jianhua Tian<sup>1</sup> · Kejian Jiang<sup>2</sup> · Jinhua Huang<sup>2</sup> · Lipeng Zhang<sup>2</sup> · Huijia Wang<sup>1,2</sup> · Bin Bao<sup>2</sup> · Yanlin Song<sup>2</sup>

Received: 21 March 2017 / Accepted: 30 May 2017 / Published online: 3 June 2017  
© Springer Science+Business Media New York 2017

**Abstract** In this report, a novel and facile in situ gas–solid reaction method has been developed for the deposition of CdS quantum-dots (QDs) on a mesoscopic TiO<sub>2</sub> film. In the approach, cadmium nitrate solution was first coated on mesoporous TiO<sub>2</sub> films, and subsequently transformed into CdS QDs (with size about 2–3 nm) by reaction with hydrogen sulfide (H<sub>2</sub>S) gas generated in a closed container at room temperature. Different from the conventional solution techniques, this method offers new opportunities for rapid and facile deposition of CdS QD-coated TiO<sub>2</sub> films without the introduction of the by-products. With the CdS QDs-decorated TiO<sub>2</sub> active electrodes, the liquid and solid solar cells were fabricated with power conversion efficiencies (*PCEs*) of 1.90 and 0.80%, respectively.

## 1 Introduction

Semiconductor quantum dots (QDs) have attracted great attention due to their unique properties, such as tunable band gaps on account of the quantum confinement effect,

high absorption coefficients than most organic dyes, large intrinsic dipole moment, and multiple exciton generation (MEG) [1]. In comparison with conventional ruthenium dyes and organic dyes [2, 3], semiconductor QDs would be commendable alternatives for quantum dot-sensitized solar cells (QDSSCs) in terms of light-harvesting ability and device stability [4–6]. In the past few years, chalcogenide QDs such as CdS [7–9], CdSe [10–12], PbS [13, 14], and Sb<sub>2</sub>S<sub>3</sub> [15, 16] have been extensively investigated and employed in QDSSCs, and high efficiency up to 7% was achieved [17].

So far, various approaches have been employed for fabrication of QD-decorated mesoporous semiconductor electrodes (typically, TiO<sub>2</sub>) [18, 19]. Generally, these approaches can be categorized into two major methods: in situ fabrication, and attachment of pre-synthesized colloidal QDs [20]. Among them, the in situ methods are extensively investigated for QD-decorated TiO<sub>2</sub> films [21], including chemical bath deposition (CBD) [22–25], and successive ionic layer adsorption and reaction (SILAR) [26–29]. In the CBD method, nucleation and growth of QDs proceed on the TiO<sub>2</sub> surface in one bath containing both the cationic and anionic ions in solutions. In spite of being facile and low cost, the CBD technique usually takes a long time (usually several hours) for the deposition, and the quality of QD-coated films strongly depends on the ionic concentration, temperature and pH value during the deposition [30]. In addition, a large amount of QDs also proceeds on the undesired surface of the bath container [31]. Moreover, the formation of relevant oxides cannot be avoided by the conventional aqueous phase CBD technique, which will deteriorate the device performance. The SILAR method, as an extension of the CBD technique, separates the QD growth through repetitive cycles of cationic and anionic precursors in

---

**Electronic supplementary material** The online version of this article (doi:10.1007/s10854-017-7263-1) contains supplementary material, which is available to authorized users.

---

✉ Kejian Jiang  
kjjiang@iccas.ac.cn

✉ Yanlin Song  
ylsong@iccas.ac.cn

<sup>1</sup> School of Chemical Engineering and Technology, Tianjin University, Tianjin 300072, People's Republic of China

<sup>2</sup> Key Laboratory of Green Printing, Institute of Chemistry, Chinese Academy of Sciences, Beijing 100190, People's Republic of China

two separated containers [29]. This technique benefits homogenous distribution, high coverage degree, and precise thickness of QD film on the substrates. However, the process is relatively low growth rate with multi-steps.

In our previous report, CdS QD-polymer nanocomposite was prepared by reaction of a cadmium source and H<sub>2</sub>S gas [32]. Herein, a modified technique is employed for fabrication of CdS QD-sensitized TiO<sub>2</sub> films: cadmium nitrate is first spin-coated from solution on the TiO<sub>2</sub> film, and subsequently transformed into CdS QDs by further reaction with H<sub>2</sub>S gas. The reaction occurs as soon as the two components come into contact, resulting in CdS QDs covered on the TiO<sub>2</sub> films. The QDs-decorated film was used as a photo anode in combination with a P3HT hole transport layer or liquid electrolyte for solid or liquid QDSSCs, respectively, with initial power conversion efficiencies of 0.80% for solid QDSSCs and 1.90% for the liquid counterpart under AM 1.5G illumination. This technique provides a new approach for rapid and facile fabrication of sulfide semiconductor QDs-sensitized electrodes.

## 2 Experimental details

### 2.1 Fabrication of TiO<sub>2</sub> films

For the fabrication of the TiO<sub>2</sub> thin films, fluorine-doped SnO<sub>2</sub> (FTO) substrates with a resistivity of  $\sim 10 \Omega \text{ cm}^{-1}$  were cleaned with detergent, then ultrasonic treatment in deionized water, ethanol and acetone successively, and then blow-dried by nitrogen gas. 0.15 and 0.3 M titanium (diisopropoxide) *bis*(2,4-pentanedionate) (dissolved in *n*-butanol) were spin coated on the FTO substrate respectively and heated on hot plate to form dense titanium dioxide as barrier layer to prevent short circuiting. The TiO<sub>2</sub> paste was prepared by dispersing 20 nm-sized TiO<sub>2</sub> particles and 60 nm-sized TiO<sub>2</sub> particles (Aladdin, T104936) with a weight ratio of 7:3, which can provide larger pore sizes for the deposition of CdS QDs and efficient penetration of hole transport polymer P3HT and electrolyte, and at the same time support large specific surface area for CdS QDs decoration [33]. Mesoscopic TiO<sub>2</sub> films were prepared by spin coating or blading of TiO<sub>2</sub> paste on the substrates for solid or liquid QDSSCs, followed by calcination at 450 °C for 30 min. The resulting milky white TiO<sub>2</sub> film was further treated with an aqueous solution of 40 mM TiCl<sub>4</sub> for 30 min at 70 °C, followed by calcination again at 500 °C for 30 min [34]. Above 500 nm or 5 μm thick TiO<sub>2</sub> films were employed for the fabrication of CdS QD sensitized solar cells.

### 2.2 Fabrication of CdS QD-coated TiO<sub>2</sub> films

For the fabrication of CdS QD-sensitized TiO<sub>2</sub> films, the in situ gas–solid reaction was employed, including two-step coating procedure: first, 0.3 M of Cd(NO<sub>3</sub>)<sub>2</sub>·4H<sub>2</sub>O ethanol solution (50 μl) was loaded on the mesoporous TiO<sub>2</sub> film for 10 s, then spin-coated at 2000 r.p.m. for 20 s. Notably extra 100 μl solution was added dropwise in the TiO<sub>2</sub> films during the procedure of spin. The Cd salt-coated TiO<sub>2</sub> film was then put in an enclosed glass container (10 l in volume), where a 200 ml beaker containing a mixed aqueous solution (250 ml) of 20 wt.% sodium sulfide (Na<sub>2</sub>S·9H<sub>2</sub>O) and 10 wt.% dilute sulfuric acid (H<sub>2</sub>SO<sub>4</sub>), was placed in advance for generating H<sub>2</sub>S gas. The reaction occurred quickly as soon as the two components came into contact, resulting in the color change of the TiO<sub>2</sub> film from milky white to canary yellow immediately. The color became dark rapidly, and did not change after 5 min, indicating complete reaction of the coated Cd salt with H<sub>2</sub>S, that is, the formation of CdS within the TiO<sub>2</sub> film. After 5 min, the film was taken out and washed by deionized water and then ethanol to remove the resulting by-product. All the processes were performed at room temperature under a fume hood. For simplicity, we refer to the in situ gas–solid reaction method as IS-GS throughout the manuscript.

For comparison, the optimized SILAR method was employed for the fabrication CdS-coated TiO<sub>2</sub> film according to the previous report [26]. Briefly, The identical TiO<sub>2</sub> film was dipped in 0.1 M Cd(NO<sub>3</sub>)<sub>2</sub>·4H<sub>2</sub>O ethanol solution for 30 s, rinsed with ethanol for 30 s, dipped for an additional 30 s in a 0.1 M Na<sub>2</sub>S methanol/water (7:3/v:v) solution, and then rinsed with water for 30 s. All of these processes constitute one SILAR cycle, and the process was repeated for 10 cycles to obtain the optimized loading of CdS QDs.

### 2.3 Fabrication of CdS QD-sensitized solid-state and liquid-state solar cells

For the fabrication of the solid-state sensitized solar cell, P3HT (Rieke Metals) was employed as hole transport material, which was infiltrated into the CdS QD-sensitized mesoporous TiO<sub>2</sub> film by spin coating a P3HT solution (25 mg ml<sup>-1</sup> in chlorobenzene) at 2000 rpm for 60 s in a glovebox. The samples were then annealed on a hot plate at 150 °C for 10 min, followed by slowly cooling to room temperature [35, 36]. Finally, a 60 nm thick silver (Ag) counter electrode was deposited by thermal evaporation.

For the liquid-state solar cell, the CdS-modified TiO<sub>2</sub> electrode and a Pt-coated counter electrode were sandwiched using 60 μm thick sealing material (SX-1170, Solaronix SA). 3-methoxypropionitrile solution consisting of 0.1 M lithium iodide, 0.05 M iodine, 0.6 M

1-propyl-2,3-dimethylimidazolium iodide, and 0.5 M 4-terbutylpyridine was used as redox electrolyte.

## 2.4 Characterization

The X-ray diffraction (XRD) patterns were recorded with a Bruker D8 Discover diffractometer in Bragg–Brentano mode, using Cu K $\alpha$  radiation (1.540598 Å) and a Ni  $\beta$ -filter, from  $2\theta=20^\circ$ – $60^\circ$  at a scan rate of  $2^\circ \text{ min}^{-1}$ . The morphologies (SEM) and the X-ray energy-dispersive spectrometer (EDS) of the CdS-coated TiO<sub>2</sub> film were investigated by a field-emission scanning electron microscope (JSM-7500, Japan). Transmission electron microscopy (TEM) images were acquired with a JEOL HT7700 microscope. The absorption spectra were measured using a UV–Vis spectrometer (Shimadzu UV-2600) and X-ray photoelectron spectroscopy (XPS) were performed on the Thermo Scientific ESCA Lab 250Xi using 200 W monochromated Al K $\alpha$  radiation, and 500  $\mu\text{m}$  X-ray spot was used for XPS analysis. Typically the hydrocarbon C1s line at 284.8 eV from adventitious carbon is used for energy referencing. The photocurrent–voltage ( $J$ – $V$ ) measurement

of the devices was conducted on a computer-controlled Keithley 2400 Source Measure Unit under the illumination of simulated AM 1.5 G, 100  $\text{mW cm}^{-2}$  using a xenon-lamp-based solar simulator. The external quantum efficiency ( $EQE$ ) spectra for the devices were performed using a commercial setup (PV-25 DYE, JASCO). A 300 W Xenon lamp was employed as light source for generation of a monochromatic beam. Calibrations were performed with a standard silicon photodiode.  $EQE$  is defined by  $EQE(\lambda) = hcJ_{sc}/e\phi\lambda$ , where  $h$  is Planck's constant,  $c$  is the speed of light in a vacuum,  $e$  is the electronic charge,  $\lambda$  is the wavelength in meters (m),  $J_{sc}$  is the short-circuit photocurrent density ( $\text{A m}^{-2}$ ), and  $\phi$  is the incident radiation flux ( $\text{W m}^{-2}$ ).

## 3 Results and discussion

### 3.1 Characterization of CdS QD-sensitized TiO<sub>2</sub> film

Figure 1a shows X-ray diffraction (XRD) patterns of the naked TiO<sub>2</sub> film, the CdS-coated films by IS-GS method.

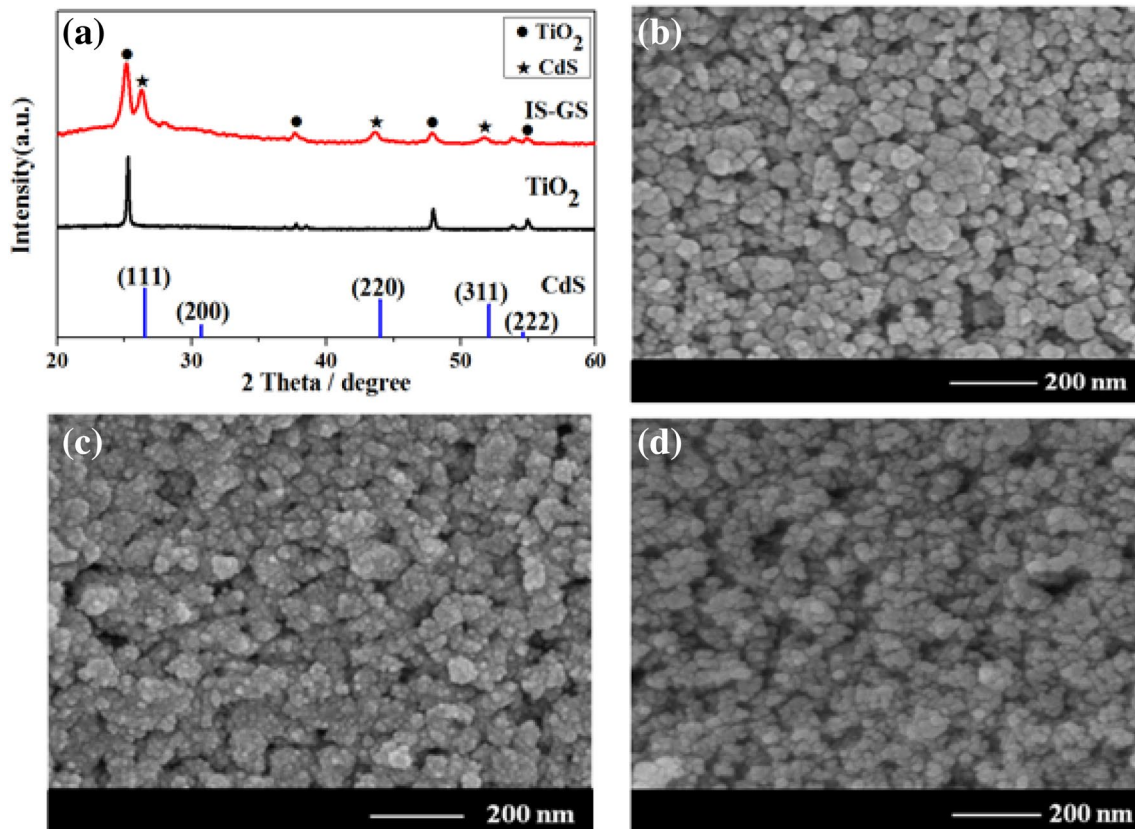


**Fig. 1** a XRD patterns of the pristine TiO<sub>2</sub> film (black), the TiO<sub>2</sub> film coated by CdS-QDs using IS-GS method (red), and cubic CdS (JCPDS 80-0019, blue), and the top-view scanning electron micro-

scope (SEM) images of the TiO<sub>2</sub> film (b), and the films coated by CdS-QDs by IS-GS (c) and SILAR (d). (Color figure online)

The vertical lines show the XRD pattern of cubic CdS (JCPDS 80-0019) with peaks at  $26.51^\circ$ ,  $43.98^\circ$ , and  $52.09^\circ$  for (111), (220) and (311) faces [37]. The peaks at the same positions were observed for the CdS-coated films by IS-GS method, and no peaks related to the oxide or cadmium salts was detected, affirming the successful deposition with pure cubic CdS phase by IS-GS method. In addition, the broad peaks imply that the deposited CdS particles have small sizes on the TiO<sub>2</sub> film.

Figure 1b–d show the top-view scanning electron microscope (SEM) images of the TiO<sub>2</sub> film, and the CdS-coated films by IS-GS and SILAR methods, respectively. The considerable difference was observed between these films. The naked TiO<sub>2</sub> film composes of ball-shaped TiO<sub>2</sub> particles with different sizes of ~20 and ~60 nm, respectively. After the CdS deposition by IS-GS, the film appears considerable dense and a large number of tiny CdS particles homogeneously distributed throughout the entire TiO<sub>2</sub> matrices. In the case of the SILAR film with optimized 10 cycles, the larger particles were observed, and the TiO<sub>2</sub> particles could not be clearly distinguished after the CdS deposition. After the CdS deposition by the two methods, the porous structural characterization of the naked TiO<sub>2</sub> films still remained, which can facilitate the penetration of the electrolyte or charge transport materials within the films. In addition, cross sectional SEM images and corresponding EDS distributions (Fig. S1) show that both Cd and S elements are uniformly distributed through the entire porous TiO<sub>2</sub> film.

In order to further probe the morphology of the CdS-coated TiO<sub>2</sub> films by the two different methods, high resolution transmission electron microscopy (HRTEM) was employed. As shown in Fig. 2, CdS QDs fabricated by IS-GS method can be distinguished as small particles, which are homogeneously decorated on the TiO<sub>2</sub> surface with crystal grain size of about 2–3 nm. The TiO<sub>2</sub> and CdS lattice fringe spacings are at 0.25 and 0.21 nm, indicating anatase phase of TiO<sub>2</sub> and cubic phase of CdS, respectively [11]. By contrast, the diameter of CdS QDs with SILAR

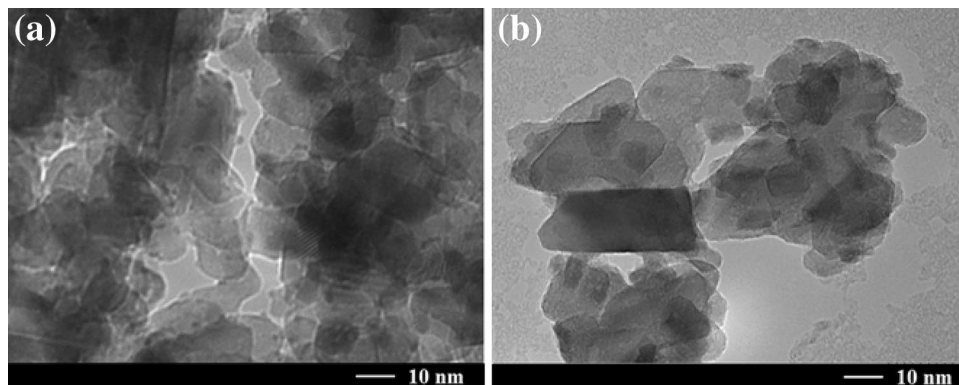
method is approximately 5–6 nm, larger than that formed by IS-GS method.

X-Ray photoelectron spectroscopy (XPS) measurement was performed to investigate the electronic structures and chemical properties of the CdS-coated TiO<sub>2</sub> films prepared by IS-GS and SILAR methods. Figure S2 illustrates the full XPS survey-scan and narrow-scan of the CdS QDs-decorated TiO<sub>2</sub> films. The peaks corresponding to Ti (2p), O (1s), S (2p) and Cd (3d) are clearly observed for both the films, attributed to the TiO<sub>2</sub> film and the CdS QDs. Figure 3 show that both the samples exhibit the peaks of S (2p<sub>3/2</sub>) (161.9 eV) and S (2p<sub>1/2</sub>) (163.0 eV), and the peaks of Cd (3d<sub>5/2</sub>) (404.9 eV) and Cd (3d<sub>3/2</sub>) (411.7 eV), corresponding to the CdS QDs coated on the TiO<sub>2</sub> films [38]. The approximate atomic ratios of Cd and S, calculated by analyzing the XPS survey scan (Supporting information Table 1), are 1:0.98 for the IS-GS sample, and 1:1.22 for the SILAR sample, indicating more pure CdS formation by IS-GS method. In fact, the SILAR sample exhibits additional peaks at 168.4 eV for S (2p<sub>3/2</sub>) and 169.5 eV S (2p<sub>1/2</sub>), that are bonded with oxygen atoms and exist in the form of SO<sub>4</sub><sup>2-</sup>, probably as CdSO<sub>4</sub> [39, 40]. This result reveals that IS-GS method offers new opportunities for deposition of CdS QD-coated TiO<sub>2</sub> films without the introduction of by-products.

### 3.2 Photovoltaic performance of CdS QD-sensitized solar cells

The CdS QDs-coated TiO<sub>2</sub> electrode was used for the fabrication of liquid and solid-state sensitized solar cells. For the liquid cells, ~5 μm thick TiO<sub>2</sub> film was employed as a scaffold for the QDs deposition. In the case of the solid-state cells, thin TiO<sub>2</sub> film (~0.5 μm) was employed due to both limited charge transport mobility of P3HT and its poor infiltration ability within the porous film as compared to the liquid counterpart. In order to explore the effect of the precursor solutions on the device performance, we chose precursor Cd(NO<sub>3</sub>)<sub>2</sub> solutions with different molar

**Fig. 2** The typical high resolution transmission electron microscopy (HRTEM) images of CdS sensitized TiO<sub>2</sub> samples fabricated by IS-GS (a) and SILAR (b) method





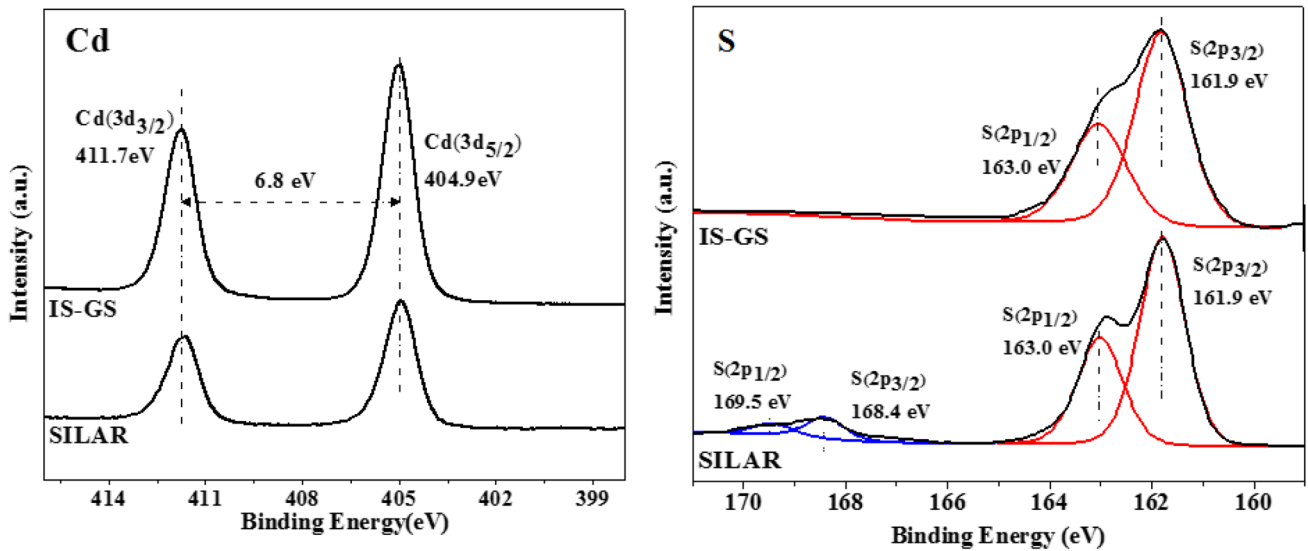


**Fig. 3** The high resolution XPS survey scan spectra of Cd 3d and S 2p for CdS-coated TiO<sub>2</sub> films using IS-GS and SILAR method

concentrations (0.1, 0.3, and 0.5 M) for the deposition of CdS QDs on the TiO<sub>2</sub> films. Figure 4 describes current–voltage characteristics of devices with the change of different concentration and preparing methods, and the specific photovoltaic performance parameters short circuit current density ( $J_{sc}$ ), open circuit potential ( $V_{oc}$ ), fill factor ( $FF$ ) and conversion efficiency ( $\eta$ ) are list in Table 1. For comparison, the photovoltaic data for the optimized SILAR device were included. For the liquid solar cells, we observed that with the increase of the precursor concentration, the  $J_{sc}$  remarkably increased from 2.92 mA cm<sup>-2</sup> for 0.1 M to 4.72 mA cm<sup>-2</sup> for 0.3 M, and slightly increased to 5.02 mA cm<sup>-2</sup> for 0.5 M. The trend would related to the enhanced light absorption ability due to more amount

of CdS formed on the TiO<sub>2</sub> film, as is evident from the absorption spectra in Fig. 5. However, we observed that the  $V_{oc}$  markedly decreased from 660 to 608 mV with the increase of the concentration from 0.3 to 0.5 M, resulting in decrease of the efficiency from 1.90 to 1.50%. The decrease in  $V_{oc}$  for the high concentration (0.5 M) may be due to high recombination rate of the over coating of the CdS. For the solid-state devices, the same trend was observed with the best efficiency (0.80%) achieved with the precursor at 0.3 M.

For the CdS QD-coated TiO<sub>2</sub> film prepared by optimized SILAR (10 cycles) method [26], the liquid device gave a  $PCE$  ( $\eta$ ) of 1.59% with a  $J_{sc}$  of 4.22 mA cm<sup>-2</sup>,  $V_{oc}$  of 0.67 V,  $FF$  of 0.56, corresponding to 1.90%, while the

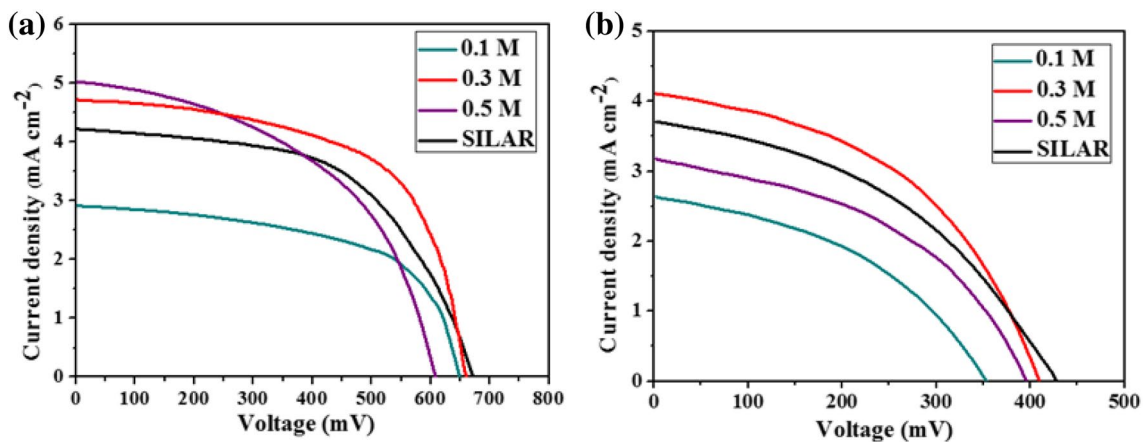


**Fig. 4** Current density–voltage ( $J$ - $V$ ) curves of CdS-coated liquid (a) and solid (b) QDSSCs using IS-GS with different concentrations of Cd(NO<sub>3</sub>)<sub>2</sub> and SILAR method under the illumination of 1 sun (AM

1.5, 100 mW cm<sup>-2</sup>) (The active area of the liquid cell is 0.1 cm<sup>2</sup> and the solid is 0.04 cm<sup>2</sup>, respectively)

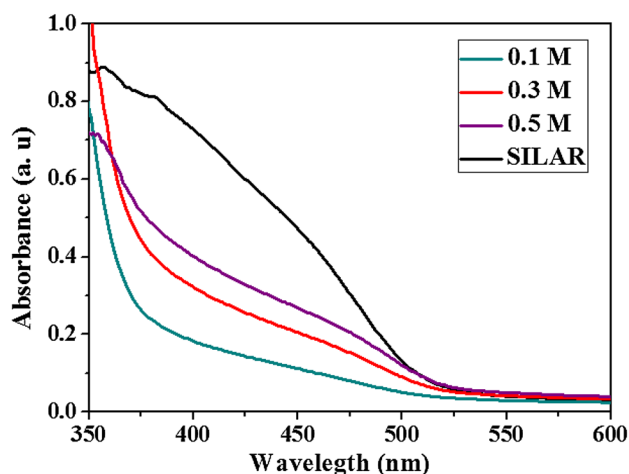


**Fig. 5** UV-vis absorption of CdS-coated TiO<sub>2</sub> films using SILAR and IS-GS methods with different concentrations of Cd(NO<sub>3</sub>)<sub>2</sub>

**Table 1** Photovoltaic parameters of liquid and solid CdS QDSSCs with IS-GS and SILAR method respectively, measured at 100 mW cm<sup>-2</sup> light intensity

Device type	Device	$J_{sc}$ (mA cm <sup>-2</sup> )	$V_{oc}$ (mV)	$FF$	$\eta$ (%)
Liquid	IS-GS-0.1	2.92	648	0.60	1.12
	IS-GS-0.3	4.72	660	0.61	1.90
	IS-GS-0.5	5.02	608	0.49	1.50
	SILAR	4.22	672	0.56	1.59
	SILAR <sup>a</sup>	4.30	681	0.63	1.84 [23]
Solid	IS-GS-0.1	2.63	354	0.42	0.39
	IS-GS-0.3	4.12	420	0.46	0.80
	IS-GS-0.5	3.17	396	0.45	0.56
	SILAR	3.70	426	0.42	0.66
	SILAR <sup>a</sup>	5.34	460	0.35	0.87 [26]

<sup>a</sup>The experimental data were quoted from references

solid-state device gave a  $PCE$  ( $\eta$ ) of 0.66% with a  $J_{sc}$  of 3.70 mA cm<sup>-2</sup>,  $V_{oc}$  of 426 mV and  $FF$  of 0.42, which are comparable with those for the CdS QDSSCs prepared by SILAR method [23, 26]. By contrast, the optimized liquid and solid-state CdS devices prepared using IS-GS method, exhibited higher efficiencies of 1.90 and 0.80%, respectively. The higher conversion efficiencies were mainly due to higher short circuit current densities. Considering the fact that the CdS QD coated TiO<sub>2</sub> film prepared by SILAR method has higher light absorption over the entire spectral region as compared with the IS-GS counterpart (Fig. 5), we speculated that the device using IS-GS method could have higher incident photon-to-electron conversion efficiency (IPCE), as is evident from Fig. 6.

Considering the facile and fast deposition of CdS QDs on TiO<sub>2</sub> film and few by-products, the IS-GS technique would provide new opportunities for the fabrication of metal sulfide semiconductor QDSSCs. It should be noted that further improvement of the device performance could be expected by optimizing the morphology and thickness of TiO<sub>2</sub> film, and employing narrow band gap semiconductors. In addition, surface treatment of the absorber or the TiO<sub>2</sub> using higher band gap materials would be necessary to inhibit the charge recombination between the hole transport material P3HT or electrolyte and TiO<sub>2</sub> (and or CdS), and improve the photo voltage and thus device performance.

## 4 Conclusion

Herein, a rapid and facile deposition method for CdS QDs on mesoporous TiO<sub>2</sub> films was developed. The process includes simple solution deposition of Cd salt, and subsequently transformed into CdS QDs through in situ

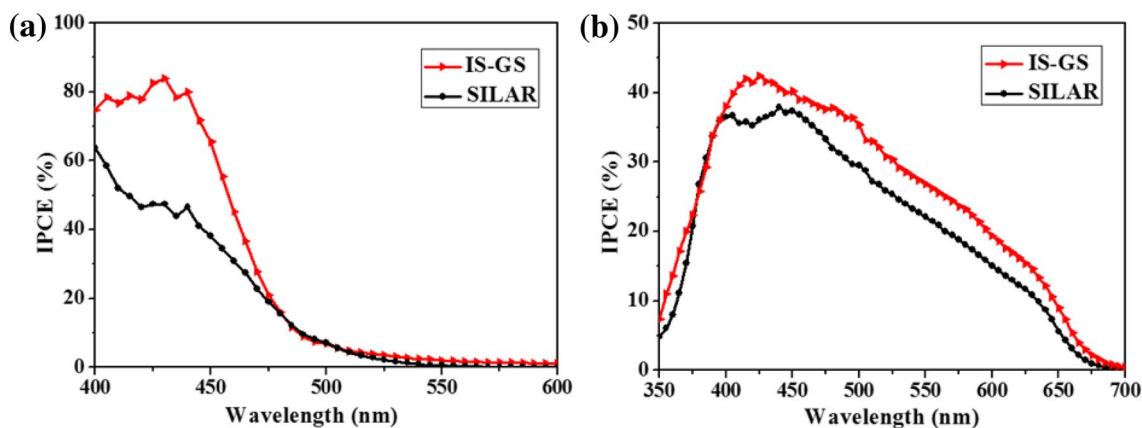


**Fig. 6** Incident photon-to-electron conversion efficiency (IPCE) spectra of the best performing liquid (a) and solid (b) devices prepared by IS-GS and SILAR method, respectively

gas–solid reaction with H<sub>2</sub>S gas with one cycle and less than 5 min. The deposited CdS QDs were homogeneous distributed on the TiO<sub>2</sub> film with particle sizes of about 2–3 nm, which are smaller than those (~5–6 nm) using conventional SILAR method. The CdS QD-sensitized liquid and solid solar cells were prepared with higher conversion efficiencies as compared with the SILAR counterpart. Our work should provide new approaches for rapid and facile fabrication of other metal sulfide semiconductor-based optoelectronic devices.

**Acknowledgements** This work was supported by the 973 Program (Nos. 2013CB933004), the National Nature Science Foundation of China (Grant Nos. 61405207, 21174149, 21572235, 51473173, 91433202 and 21221002), and the “Strategic Priority Research Program” of Chinese Academy of Sciences (Grant Nos. XDA09020000 and XDB12010200). The measurements of (XRD, SEM, HRTEM and XPS) were performed at the Center for Physicochemical Analysis and Measurements in ICCAS.

## References

- C.M. Chuang, P.R. Brown, V. Bulović, M.G. Bawendi, *Nat. Mater.* **13**, 796 (2014)
- A. Hagfeldt, G. Boschloo, L. Sun, L. Kloo, H. Pettersson, *Chem. Rev.* **110**, 6595 (2010)
- S. Mathew, A. Yella, P. Gao, R. Humphry-Baker, B.F.E. Curchod, N. Ashari-Astani, I. Tavernelli, U. Rothlisberger, M.K. Nazeeruddin, M. Gratzel, *Nat. Chem.* **6**, 242 (2014)
- P.V. Kamat, *J. Phys. Chem. Lett.* **4**, 908 (2013)
- M. Kouhnavard, S. Ikeda, N.A. Ludin, N.B.A. Khairudin, B.V. Ghaffari, M.A. Mat-Teridi, M.A. Ibrahim, S. Sepeai, K. Sopian, *Renew. Sust. Energy Rev.* **37**, 397 (2014)
- J. Duan, H. Zhang, Q. Tang, B. He, L. Yu, *J. Mater. Chem. A* **3**, 17497 (2015)
- B. Zhang, J. Zheng, X. Li, Y. Fang, L. Wang, Y. Lin, F. Pan, *Chem. Commun.* **52**, 5706 (2016)
- L. Li, X. Yang, J. Gao, H. Tian, J. Zhao, A. Hagfeldt, L. Sun, *J. Am. Chem. Soc.* **133**, 8458 (2011)
- H. Kim, H. Jeong, T.K. An, C.E. Park, K. Yong, *ACS Appl. Mat. Interfaces* **5**, 268 (2013)
- A. Kongkanand, K. Tvrđy, K. Takechi, M. Kuno, P.V. Kamat, *J. Am. Chem. Soc.* **130**, 4007 (2008)
- S.A. Pawar, D.S. Patil, H.R. Jung, J.Y. Park, S.S. Mali, C.K. Hong, J.-C. Shin, P.S. Patil, J.-H. Kim, *Electrochim. Acta.* **203**, 74 (2016)
- F.S. Ghoreishi, V. Ahmadi, M. Samadpour, *J. Power Sources* **271**, 195 (2014)
- J.-W. Lee, D.-Y. Son, T.K. Ahn, H.-W. Shin, I.Y. Kim, S.-J. Hwang, M.J. Ko, S. Sul, H. Han, N.-G. Park, *Sci. Rep.* **3**, 1050 (2013)
- S. Jiao, J. Wang, Q. Shen, Y. Li, X. Zhong, *J. Mater. Chem. A* **4**, 7214 (2016)
- S. Mushtaq, B. Ismail, M.A. Zeb, N.J.S. Kissinger, A. Zeb, *J. Alloys Compd.* **632**, 723 (2015)
- E. Zimmermann, T. Pfadler, J. Kalb, J.A. Dorman, D. Sommer, G. Hahn, J. Weickert, L. Schmidt-Mende, *Adv. Sci.* **4**, 201500059 (2015)
- A.H. Ip, S.M. Thon, S. Hoogland, O. Voznyy, D. Zhitomirsky, R. Debnath, L. Levina, L.R. Rollny, G.H. Carey, A. Fischer, K.W. Kemp, I.J. Kramer, Z. Ning, A.J. Labelle, K. Chou, A. Amassian, E.H. Sargent, *Nat. Nano.* **7**, 577 (2012)
- M.A. Halim, *J. Nanomater.* **3**, 22 (2013)
- H. Weller, *Adv. Mater.* **5**, 88 (1993)
- W. Li, X. Zhong, *J. Phys. Chem. Lett.* **6**, 796 (2015)
- J. Albero, J.N. Clifford, E. Palomares, *Coord. Chem. Rev.* **263–264**, 53 (2014)
- H. Wang, Y. Bai, H. Zhang, Z. Zhang, J. Li, L. Guo, *J. Phys. Chem. C* **114**, 16451 (2010)
- Y.-L. Lee, C.-H. Chang, *J. Power Sources* **185**, 584 (2008)
- O. Niitsoo, S.K. Sarkar, C. Pejoux, S. Rühle, D. Cahen, G. Hodes, *J. Photochem. Photobiol. A* **181**, 306 (2006)
- C.-H. Chang, Y.-L. Lee, *Appl. Phys. Lett.* **91**, 053503 (2007)
- N. Balis, V. Dracopoulos, E. Stathatos, P. Lianos, *J. Phys. Chem. C* **115**, 10911 (2011)
- P. Ardalan, T. Brennan, H.-B.-R. Lee, S. Bent, *ACS Nano* **5**, 1495 (2011)
- H. Lee, M. Wang, P. Chen, D.R. Gamelin, S.M. Zakeeruddin, M. Gratzel, M.K. Nazeeruddin, *Nano Lett.* **9**, 4221 (2009)
- E. Rabinovich, G. Hodes, *J. Phys. Chem. C* **117**, 1611 (2013)
- F. Laatar, A. Harizi, A. Smida, M. Hassen, H. Ezzaouia, *Mater. Res. Bull.* **78**, 83 (2016)
- J. Zhou, B. Song, G. Zhao, W. Dong, G. Han, *Appl. Phys. A* **107**, 321 (2012)
- B. Bao, M. Li, Y. Li, J. Jiang, Z. Gu, X. Zhang, L. Jiang, Y. Song, *Small* **11**, 1649 (2015)
- Q. Zhang, X. Guo, X. Huang, S. Huang, D. Li, Y. Luo, Q. Shen, T. Toyoda, Q. Meng, *Phys. Chem. Chem. Phys.* **13**, 4659 (2011)
- J. Kim, H. Choi, C. Nahm, C. Kim, S. Nam, S. Kang, D.-R. Jung, J.I. Kim, J. Kang, B. Park, *J. Power Sources* **220**, 108 (2012)
- K.-J. Jiang, K. Manseki, Y.-H. Yu, N. Masaki, K. Suzuki, Y. Song, S. Yanagida, *Adv. Funct. Mater.* **19**, 2481 (2009)
- J. Qian, Q.-S. Liu, G. Li, K.-J. Jiang, L.-M. Yang, Y. Song, *Chem. Commun.* **47**, 6461 (2011)
- Q. Cui, C. Liu, F. Wu, W. Yue, Z. Qiu, H. Zhang, F. Gao, W. Shen, M. Wang, *J. Phys. Chem. C* **117**, 5626 (2013)
- S.S. Mali, C.S. Shim, H. Kim, C.K. Hong, *Ceram. Int.* **42**, 1973 (2016)
- Y.C. Choi, D.U. Lee, J.H. Noh, E.K. Kim, S.I. Seok, *Adv. Funct. Mater.* **24**, 3587 (2014)
- M. Stoev, A. Katerski, *J. Mater. Chem.* **6**, 377 (1996)